Road Materials and Pavement Design

ISSN: (Print) (Online) Journal homepage: https://www.tandfonline.com/loi/trmp20

# Impact of air voids and environmental temperature of asphalt concrete on black ice

**Tam Minh Phan, Min-Seok Jang, Jung-Woo Seo, Jae-Hyeong Yoon, Dae-Wook Park & Tri Ho Minh Le**

**To cite this article:** Tam Minh Phan, Min-Seok Jang, Jung-Woo Seo, Jae-Hyeong Yoon, Dae-Wook Park & Tri Ho Minh Le (2023): Impact of air voids and environmental temperature of asphalt concrete on black ice, Road Materials and Pavement Design, DOI: 10.1080/14680629.2023.2180293

**To link to this article:** https://doi.org/10.1080/14680629.2023.2180293

Published online: 22 Feb 2023.

ROAD MATERIALS AND PAVEMENT DESIGN
https://doi.org/10.1080/14680629.2023.2180293



# Impact of air voids and environmental temperature of asphalt concrete on black ice

Tam Minh Phan [a], Min-Seok Jang[b], Jung-Woo Seo[a], Jae-Hyeong Yoon[a], Dae-Wook Park[a] and Tri Ho Minh Le[c]

[a]Department of Civil and Environmental Engineering, Kunsan National University, Gunsan, Republic of Korea; [b]Department of Computer Information Engineering, Kunsan National University, Gunsan, Republic of Korea; [c]Faculty of Civil Engineering, Nguyen Tat Thanh University, Ho Chi Minh City, Vietnam

**ABSTRACT**
This study investigates two methods for detecting black ice, a hazardous thin layer of ice on road surfaces. The rain sensor and deep learning methods were explored, while considering the influence of environmental conditions, such as temperature, humidity, and air voids in asphalt concrete, on black ice formation. Results from the rain sensor method showed that the electrical resistance involved cooling time and reached a constant value when black ice was formed. Lower air voids in asphalt concrete led to a higher chance of black ice formation, while humidity had a negligible effect. A vehicle module for detecting black ice was successfully developed using deep learning with 90% accuracy. Furthermore, experiments using infrared heating confirmed that environmental temperature affects the melting time and melting area of black ice. These findings can improve safety for drivers and help with route planning when travelling on black ice roads.

**ARTICLE HISTORY**
Received 7 September 2022
Accepted 9 February 2023

**KEYWORDS**
Asphalt concrete; black ice detection; rain sensor; air voids; infrared heating; deep learning

## Introduction

In cool regions, black ice happens when a thin coating of ice is formed on the road surface. Once black ice forms on the road surface, it is difficult to recognise due to its transparent property. Black ice strongly reduces the friction of tyre-road and road surface, thus resulting in dangerous driving (Minh Phan et al., 2021). When black ice happens, the road surface is more slippery, compared to the snow road surface and dry road surface, black ice road is 6 and 14 times more slippery. In South Korea, black ice caused 706 deaths due to car accidents from 2014 to 2018. Meanwhiles, the number of deaths caused by snow was four times lower (Kim Hyun-bin, 2019). Therefore, the detection of black ice and melting black ice are hot topics that attracted many researchers in recent years. An appropriate detection not only improves the concentration of drivers while driving but also provides a fast and effective response to prevent traffic accidents.

Several different sensor techniques have been developed with the specific objective to detect road surface conditions. Ma and Ruan developed a method to detect black ice on road surfaces using multiwavelength (e.g. 1310, 1430, and 1550 nm), then calculated backscattering power under certain conditions of road (Ma & Ruan, 2020). Casselgren et al. built a detection system based on different wavelength absorption properties of dry asphalt, water and snow (Casselgren et al., 2012). The system included laser emitters, photodetectors and signal processing (Valldorf & Gessner, 2007). Another research used a near-infrared LED system to recognise road surface conditions (Zhang et al., 2022).

**CONTACT** Dae-Wook Park dpark@kunsan.ac.kr

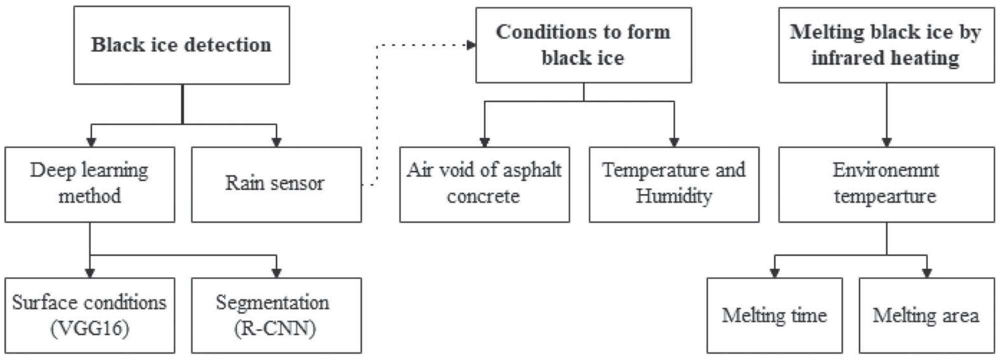


**Figure 1.** Research flowchart.

Although the detection of road conditions has been developed in most research, the detection system may be affected by the surrounding environment as lights from vehicles. Thus, the installation cost is quite expensive. Therefore, the current study aims to develop a method to detect black ice using a rain sensor with a minimised environmental influence.

With regard to the integration of object detection techniques by using the deep learning method, remarkable success in various fields has been reported such as system operation, high-end manufacturing, and road deterioration classification (Singh, 2018). Tong et al. (2018) used deep convolutional neural networks to recognise cracks in asphalt pavement. A deep learning approach has been used in Majidifard's study to predict the Hamburg rutting curve (Majidifard et al., 2021). On black ice detection, H. Lee et al. (2020) and H. Lee et al. (2020) have presented the application of a convolution neural network in the classification of black ice zone to reduce car accidents. Despite black ice detection having attracted many researchers, research on the effect of asphalt properties and environmental conditions on black ice formation is still limited. Therefore, air voids and environmental conditions are focused on in this study.

Nowadays, many methods have been developed to melt snow/ice on the road surface. For example, a heating tube system was introduced in the research of Zhao et al. (2021). However, a heating tube system may consume a huge energy and exhaust carbon dioxide to the environment. Meanwhile, using road salt may populate the environment and reduce the performance of asphalt concrete (Szklarek et al., 2022). Several studies used additives to improve the thermal properties of asphalt mixture resulting in snow melting (Han et al., 2022; Vo et al., 2015). The research from Phan et al. (2022) used micro-encapsulated phase change material to delay black ice formation, however, the price is quite expensive. Among them, the infrared heating system is considered an effective method due to its easy installation, reducing energy consumption as well.

This study aims to evaluate the effect of air void, and environmental conditions on the formation process of black ice. A method to detect black ice by the rain sensor was introduced as well as detecting black ice in real time using deep learning. An automatic vehicle was developed to collect road images for training purposes. The research also aims to generate effective methods to build the adaptive deep learning model which can be applied in various environmental conditions. In addition, melting black ice using infrared was also considered. Overall, the current study provides an overview of the black ice formation process and melting black ice using infrared heating as shown in Figure 1.

## Test methods

### *Methods to detect black ice*

#### *Detect black ice by the rain sensor*

As shown in Figure 2, the rain sensor consists a series of exposed copper traces, which act as a variable resistor whose resistance varies according to the amount of water on its surface. This resistance

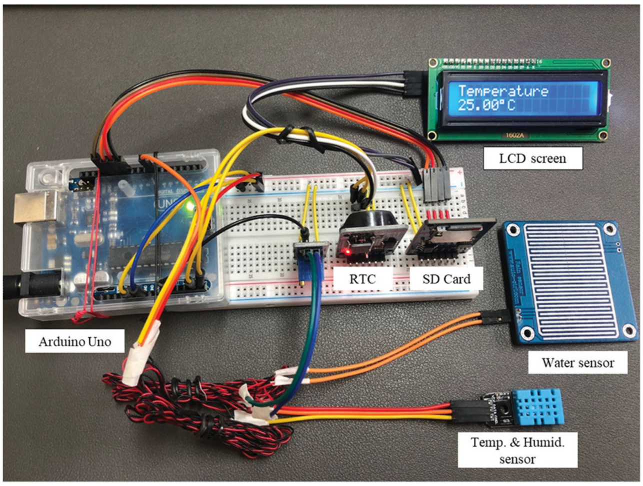


**Figure 2.** Rain sensor and Arduino circuit.

**Table 1.** Test and train images.

| | Dry condition | Wet condition | Black ice condition |
|---|---|---|---|
| Train | 1772 | 1548 | 1995 |
| Validation | 455 | 392 | 592 |

is inversely proportional to the amount of water. Therefore, more water on the surface leads to better conductivity, resulting in a lower resistance (Arduino, 2019). In contrast, less water on the surface results in poor conductivity, causing a higher resistance. In general, these traces are not connected to each other, however, bridged by water or ice. Utilisation of different electric conductivity between ice and water (Okada et al., 2021), a rain sensor is used to detect the transition from water to ice. Prior to detecting black ice formation in asphalt concrete, the behaviour of the rain sensor under water-ice transformation was examined.

The sensing pad was fully covered by 2 mm of water. Then, the water-sensing pad was placed in an incubator and conditioned at −5, −10, and −15°C for 1 h. The rain sensor was integrated with a data logger using Arduino Uno. The circuit of the system is shown in Figure 2. The system includes an Arduino Uno microcontroller, RTC (real-time clock) module, microSD card module, temperature and humidity sensor, and rain sensor. During the experiment, the time and electrical resistance values of the rain sensor were recorded by the Arduino controller.

## *Detect black ice by deep learning model*

A module was developed to collect road surface images for the deep learning model. Three road conditions were considered, including dry, wet and black ice as shown in Figure 3. In this study, a total of 6074 images were used for the training and testing model as shown Table 1.

The collected images were trained using VGGNet-one of the CNN (convolutional neural network) algorithms. VGGNet is a CNN model created by Karen Simonyan and Andrew Zisserman. They recommended that the depth of the network plays an important role in the good performance of the model. The filter size of VGGNet consists of a convolutional layer of $3 \times 3$, stride of 1, zero padding of 1. A Max-pool with a filter size of $2 \times 2$ is used as a pooling layer (Simonyan, 2015). Afterward, a mobile application was developed based on the trained model.

Subsequently, the Faster RCNN was developed in this research for black ice detection and safety classification in the actual pavement. The Faster RCNN model was developed from three main components including the Backbone network, Region network and Box Head. The properties of the input

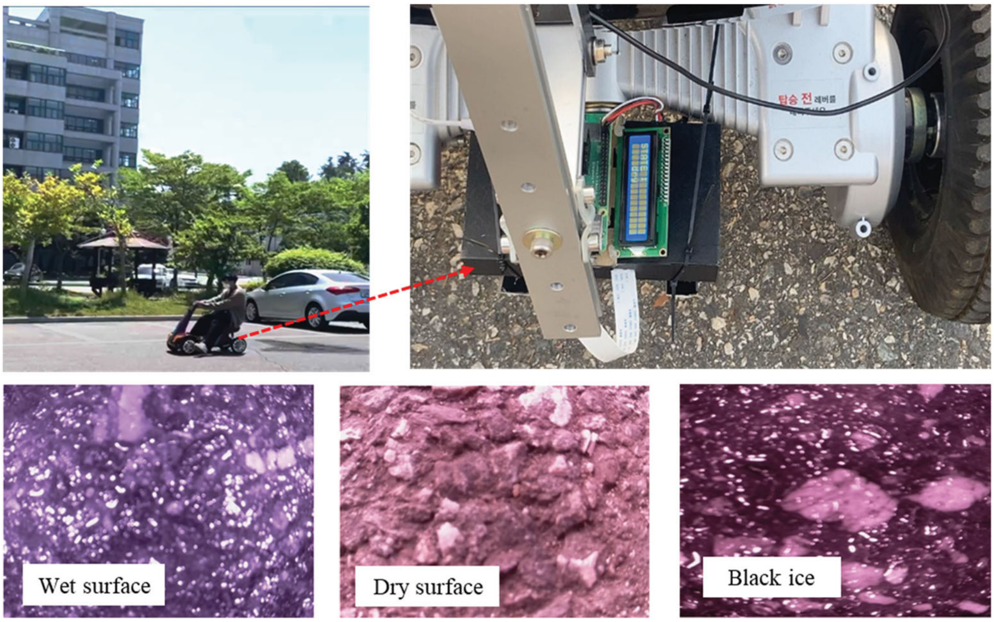


**Figure 3.** Images collected vehicle and road surface conditions.

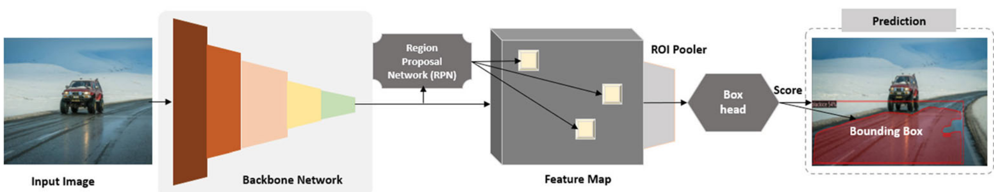


**Figure 4.** Faster R-CNN model.

image were first extracted from the Backbone. Then, they were transferred to the Region network to detect the object. The box identifications and bounding box localisation were predicted through the Box Head zone. The modelling of Faster RCNN is shown in Figure 4. Although slight customisation of the Faster R-CNN model was performed by tuning up some hyper-parameters, the default configuration of the pre-trained model was maintained in this study. Three types of Image Segmentation models (FP50-3XN, R101-FPN, and X101-FPN) were used in this research to figure out the optimum model having acceptable training time (Pham et al., 2014).

The deep learning models in this study were qualitatively evaluated based on the intersection over union (IoU) score as presented in Equation (1). In this case, if IoU $\geq 0.5$, then it is a match and vice versa.

$$IoU = \frac{area(Pb \cap Gb)}{area(Pb \cup Gb)} \tag{1}$$

where $Pb$: predicted box; Gb: ground-truth; $area(Pb \cap Gb)$: means the areas of the intersection between the two boxes, and $area(Pb \cup Gb)$: means the areas of the union between the two boxes.

Figure 5 and Table 2 summarise the classification of the dataset. The image system was developed from the two types of pavement and various weather conditions. In this research, the dataset was developed through Image Capturing by a lab car's camera, YouTube, and Google image search. All images are pre-processed to ensure detecting efficiency.

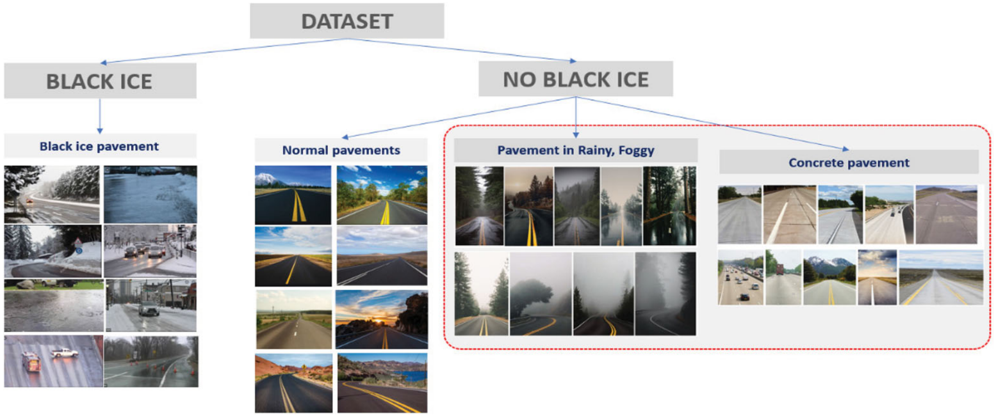


**Figure 5.** Dataset of black ice from multiple types of pavements.

**Table 2.** Summary of dataset composition (number of image data).

| Class | Train data | Validation data | Test data | Total |
|---|---|---|---|---|
| Black ice | 8000 | 2000 | 2000 | 12,000 |
| Safe (no black ice) | 8000 | 2000 | 2000 | 12,000 |

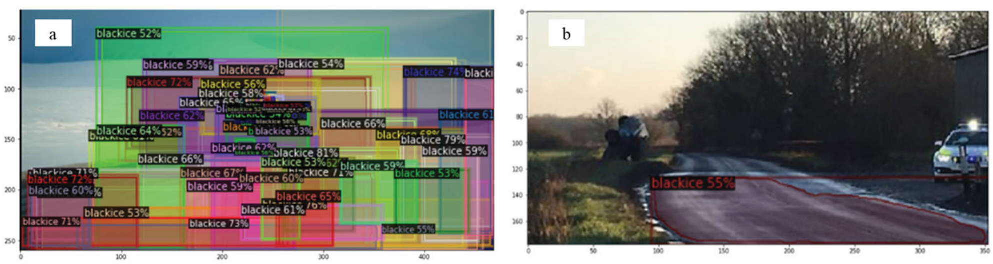


**Figure 6.** The concept of black ice detection by using image segmentation (the number (%) shown in the pictures indicates the probability of black ice).

Currently, there is a lack of quality images of black ice formed on the pavement. Therefore, data augmentation is a crucial step to diversify the limited dataset. Up to 10,000 pieces of each class were then augmented and constructed through the application of the ImageDataGenerator function. In order to increase the variety of the black ice on pavements, the augmentation steps include multiple popular tools from position augmentation (random flipping, scaling, rotating, cropping, padding) to colour augmentation (random brightness, contrast, saturation). Then, 80% of the augmented data were classified into training data and the remaining 20% was designed as validation data. Based on suggestions from related research, the over-augmentation process may lead to a significant increase in the training iteration for convergence. Therefore, the efficiency of the augmentation methods is discussed in the following section.

The concept of the bounding box for potholes and black ice detection using Faster R-CNN involves two main steps. Multiple bounding boxes were first applied with probability (Figure 6(a)). Then, refining the best bounding box generates the name of the object (Figure 6(b)).

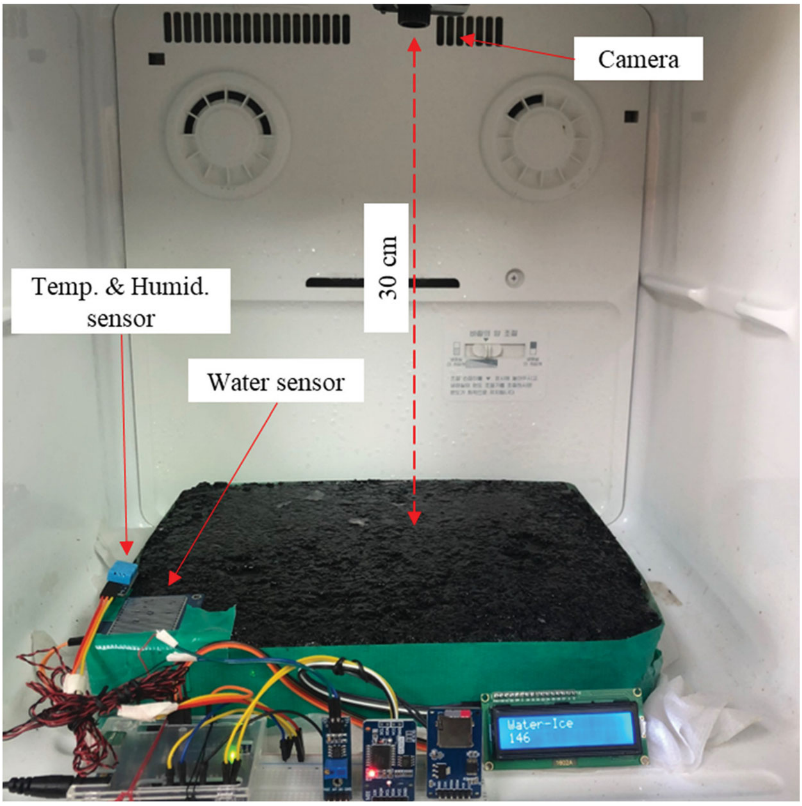


**Figure 7.** Test set-up and Arduino circuit with sensors.

## *Conditions to form black ice*

After successfully evaluating the behaviour of the rain sensor under transformation from water to ice, the rain sensor was embedded into the asphalt concrete slab. The rain sensor was embedded on the surface of the asphalt concrete slab as shown in Figure 7. In this experiment, the humidity sensor, temperature sensor and rain sensor were controlled throughout using an Arduino Uno microcontroller. In addition, the surface conditions of the asphalt concrete slab were captured every minute to confirm the formation of black ice. The test set-up is illustrated in Figure 7. Several conditions to form black ice were considered, including temperature, humidity and air voids of the asphalt slab.

### *Temperature and humidity*

This test aims to measure the influence of environmental temperature on black ice formation. Once, the temperature drops below 0°C, water changes from a liquid to a solid. Therefore, this experiment is considered to test at three temperatures, including −5°C, −10°C, and −15°C. In addition, three humidity values were considered, which were 60%, 80% and 100%. The temperature and humidity were controlled by an incubator. In this test, the wind speed was controlled at 2 m/s. During the experiment process, the resistance values of the rain sensor were recorded, and the surface conditions were captured every minute using a camera as shown in Figure 7.

### *Air voids of asphalt concrete*

Water retained on the surface was also an important factor that affects the black ice formation process. Therefore, several air voids of asphalt concrete were examined in this experiment. Three asphalt concrete slabs with different air voids content were used, including 4%, 10% and 10% with coating as

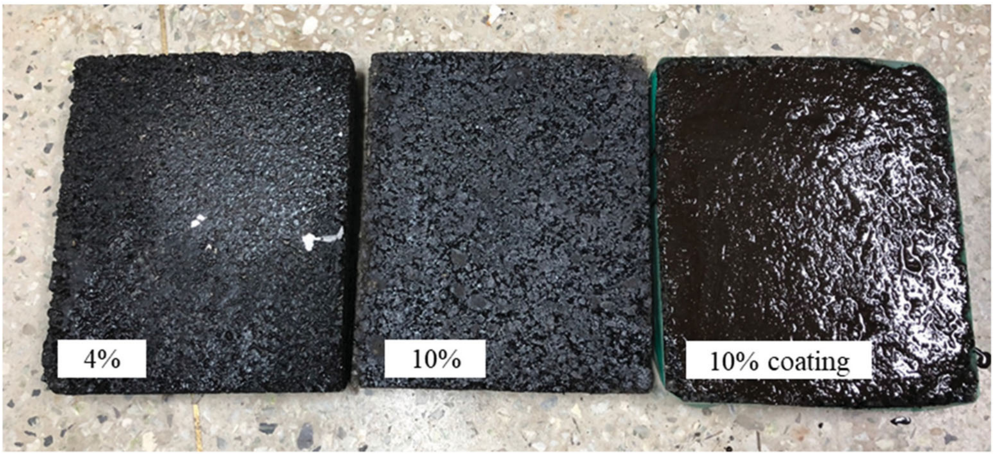


**Figure 8.** Asphalt slab with 4%, 10%, and 10% air voids with coating surface.

**Table 3.** Size gradation of aggregate

| Sieve size (mm) | 19 | 12.5 | 9.5 | 4.75 | 2.36 | 0.6 | 0.3 | 0.15 | 0.075 |
|---|---|---|---|---|---|---|---|---|---|
| Percent passing (%) | 100 | 98 | 86 | 60 | 45 | 23 | 14 | 8 | 3 |

displayed in Figure 8. In this study, the aggregates, including coarse, fine and mineral were made from limestone. Table 3 shows the size gradation of aggregate. The PG 64-22 binder was used for all asphalt mixtures with an optimum binder content of 5.4%. The surface was coated with asphalt emulsion, then conditioned in an ambient environment for 48 h before testing. An amount of 0.2-l water (equivalent to 2 mm water on the surface) was sprayed on the surface of the asphalt concrete slab. It should be noted that sprayed water was initially cooled at 1°C for 4 h. The surface conditions of the asphalt slab at 0, 20 and 60 min were captured using a camera.

## *Melting black ice by infrared heating*

This test aims to melt artificial black ice with an infrared bulb. A 100 W-infrared bulb was used in this experiment. It should be noted that control of a 2-mm layer of black ice is quite hard, therefore a 5-mm thickness of black ice was considered. Firstly, four beams having a size of $5 \times 10 \times 100$ mm were immersed in 5 mm water as shown in Figure 9. The thermocouple was glued to the surface of the concrete slab to record surface temperature during the melting process. The asphalt concrete slab was flipped for slab surface contact with the water surface to ensure the black ice thickness was 5 mm. Afterward, the sample was cured in an incubator at −18°C for 24 h prior to infrared testing. The set-up of the infrared heating test is shown in Figure 10. An infrared bulb was placed 30 cm over the surface of black ice. The surface conditions were captured every minute by a camera, which is connected to a computer. To evaluate the effect of the environment, three temperatures were considered, including −5°C, −10°C and −15°C.

ANSYS 2021-R1 program was employed to simulate the melting of black ice using an infrared bulb. Table 4 shows the thermal properties of the asphalt layer and ice layer. In this simulation, transient heat transfer is used to simulate the ice melting process. The simulation considered three modes of heat transfer, including conduction (Equation (2)), convection between the ice layer and the surrounding environment (Equation (3)) and radiation between infrared and ice layer (Equation (4)). The surface temperature of the infrared bulb was measured using an infrared camera as shown in Figure 10(a).

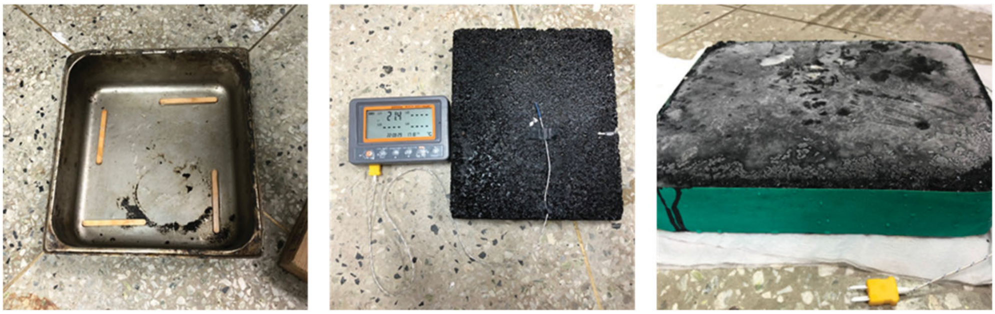

**Figure 9.** Artificial black ice on surface of asphalt concrete slab.

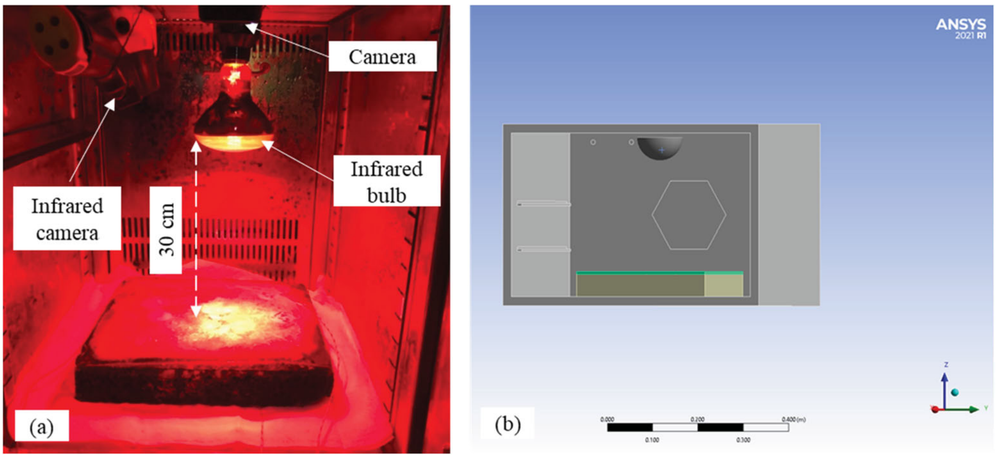


**Figure 10.** Infrared melting test set-up (a) and finite element analysis model (b).

**Table 4.** Thermal properties of ice and asphalt concrete (Vo et al., 2015)

| | Thickness (mm) | Density (kg/m$^3$) | Thermal conductivity (W/mK) | Specific heat (J/kg K) |
|---|---|---|---|---|
| Ice | 5 | 997 | 0.58 | 2180 |
| Asphalt concrete | 50 | 2350 | 1.83 | 920 |

The finite element analysis model is displayed in Figure 10(b).

$$k\left(\frac{\partial^2 T}{\partial x}+\frac{\partial^2 T}{\partial y}+\frac{\partial^2 T}{\partial z}\right)=\rho C\frac{\partial T}{\partial t} \tag{2}$$

$$q_{conv}=hA(T_s-T_\infty) \tag{3}$$

$$q_{rad}=\sigma AF_{ij}({T_i}^4-{T_j}^4) \tag{4}$$

where $k$: thermal conductivity (W/mK), $\rho$: density (kg/m$^3$), $C$: specific heat (J/kgK), $h$: convection parameter; $A$: surface area (m$^2$), and $\sigma$: Stefan–Boltzmann constant ($5.76\times10^{-8}$ kg/s$^3$ K$^4$).

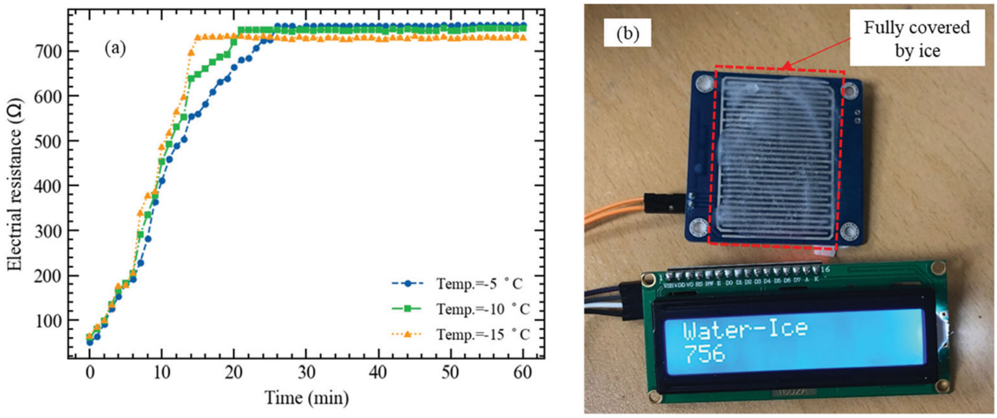


**Figure 11.** Resistance of rain sensor (a) and ice on the rain sensor (b).

## Results and discussions

### *Methods to detect black ice*

The results of the rain sensor during the freezing time are shown in Figure 11. Overall, the resistance value of the rain sensor increased with cooling time. The electrical resistance of ice was higher than that of water at the same temperature and pressure. This phenomenon can be explained by ice containing fewer ions than liquid (Bradley, 1957; Okada et al., 2021). Figure 11(a) shows that the resistance values of the rain sensor gradually increased until it reached a steady value. Three different temperatures were considered such as −5°C, −10°C and −15°C. The results indicated the lower temperature could reach a faster steady value. In other words, lower temperatures acquired faster ice formation. Based on this outcome, the black ice formation can be predicted. As shown in Figure 11(b), when the ice was fully formed on the surface of the rain sensor, the reading value was 756°CΩ.

Regarding the deep learning method, the number of epochs to train the dataset was 20. Epoch refers to the number of times the entire training data had passed through the neural network. The results from Figure 12(a) show that the accuracy of the training process was 98% while the accuracy of the test process was 90%. Due to the limitation of a small dataset, which was 6000 images, the loss rate of the test set did not decrease, and the learning was stopped by repeating up and down. After successfully training a deep learning model to detect black ice, a mobile application was developed as shown in Figure 12(b). The Raspberry processing unit determines the road surface condition and sends it to the server, and the mobile application continuously received data from the server. The black ice area was displayed as red marked, the warning as yellow, and the safety road as blue colour. Besides determining current road conditions, collected images were stored and used to train further model.

The RCNN deep learning model was evaluated as shown in the performance indicators in Figure 13. Overall, the accuracy indicator reveals that the black ice detection was acceptable. The results indicated that the accuracy of the training dataset was increased sharply in the first 500 iterations. After that the training accuracy slightly reaches the optimum level. Modifications in the programming structure have slightly improved efficiency in the train results. The trained results show that the gap between different image segmentation models is neglectable. The final average value of accuracy was 97% indicating that the learning effectiveness was adaptable for predicting black ice.

The results indicated that it is possible to detect black ice on the pavement as shown in Figure 14. The pavement type and the weather conditions may play a crucial role in the detection accuracy as shown in Figure 15. For example, when the pavement type is concrete, the white colour of the pavement may lead to the wrong labelling of the model (Figure 16). Under rainy and foggy weather, the impact of pavement type becomes neglectable due to the darker colour of concrete pavement

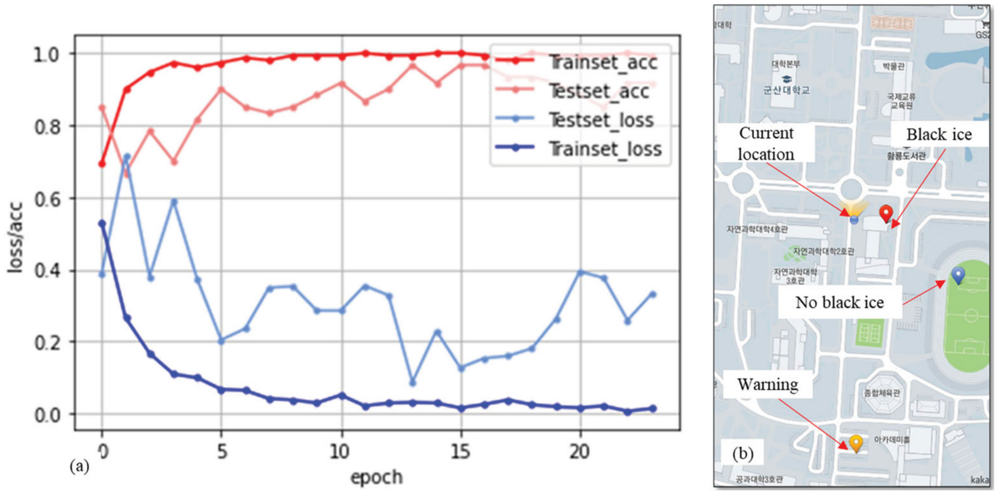


**Figure 12.** Training accuracy (a) and mobile application (b).

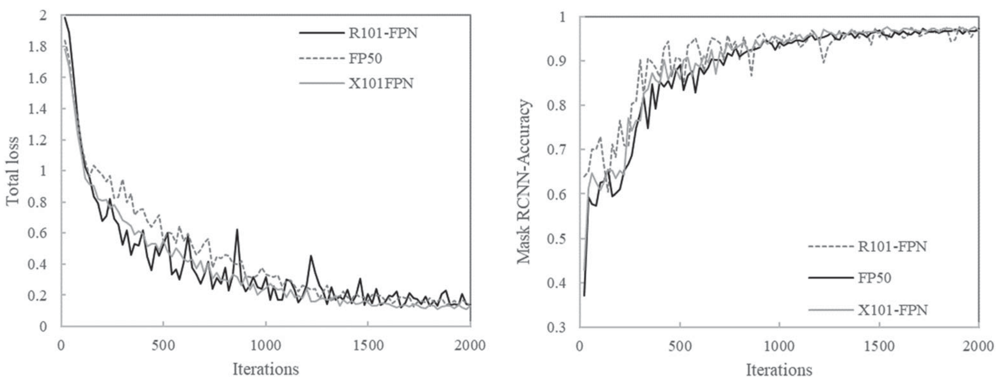


**Figure 13.** Results of learning from different image segmentation models.

under this weather condition. Especially, under foggy weather, the wet and glossy pavement leads to a huge drop in the precision index. This issue may be resolved by improving the dataset in these conditions, integrating the GPS, and applying weather forecast data to enhance the decision-making process.

## *Conditions to form black ice*

Figure 17 illustrates the relationship between humidity and temperature and black ice formation. In general, humidity lightly contributed to the formation process of black ice. The higher humidity could reduce electrical resistance, however, the effect on time to make black ice was negligible. Three different humidity required around 20 min to form black ice. The lower humidity may affect the amount of water on the sensor, lower humidity could lightly reduce the amount of rain sensor thus resulting in a higher resistance value during the freezing process. In contrast, the temperature mainly affected the time that makes black ice. The lower environment temperature led to faster black ice formation. At −5°C, −10°C and −15°C, the time to make black ice was 25, 20, and 17 min, respectively.

Figure 18 shows the influence of air voids of asphalt slabs on the black ice formation process. In the scope of this study, three different asphalt slabs were considered, including 4%, 10% and 10%


**Figure 14.** Black ice detection results of the trained model.

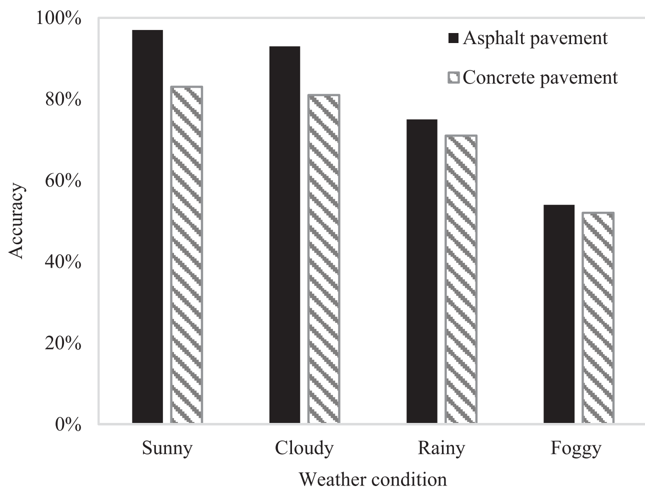


**Figure 15.** The overall accuracy of the trained model under different conditions.

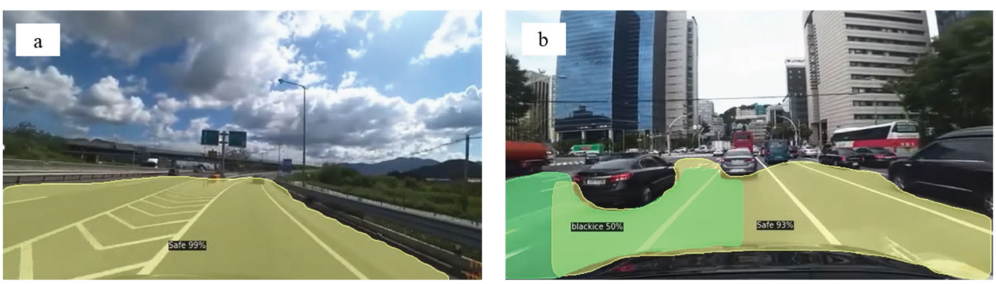


**Figure 16.** Safe zone (a) and merged results due to lack of dataset (b.)

with surface coating. The temperature was controlled at −5°C and humidity of 100%, wind speed of 2 m/s. The results show that water retained on the surface of the sample with 10% air voids disappeared after 20 min. Therefore, black ice formation was not recorded during the further process. Sample with 4% air voids, the water retained on the surface partly remained, resulting in partly black ice being recorded. The higher air voids lead to the faster water absorbed into the asphalt concrete

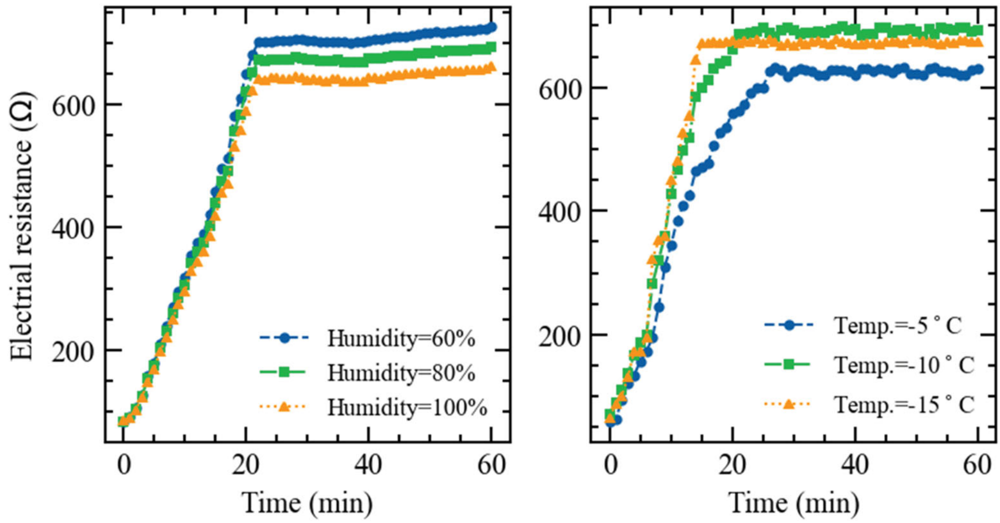


**Figure 17.** Effect of humidity and temperature on black ice formation process.

lab, resulting in no black ice recorded. Besides, the water of sample 10% with coating surface fully remained, hence, black ice was fully recorded on the slab surface as displayed in Figure 18. Overall, the higher air voids in asphalt concrete could reduce the chance of black ice formation. In other words, the water retained on the surface of asphalt concrete was considered a priority condition to form black ice.

### *Melting black ice by infrared heating*

The results of melting black ice by infrared heating are displayed in Figure 19. Three environment temperatures were considered, including −5°C, −10°C and −15 °C. The melting time was assumed as the time temperature of the embedded thermocouple was higher than 0°C. In general, low-environment temperature could reduce the influence of infrared heating. The lower temperature decreased the melting area of black ice, which was 283, 133, and 64 $cm^2$ corresponding to −5°C, −10°C, and −15°C, respectively. Similar to the melting area, melting time was increased with a decrease in temperature. The melting time was 21, 61, and 112 min corresponding to −5°C, −10°C and −15°C, respectively. This can be explained by the lower environment temperature decreased surface temperature of the infrared bulb, resulting in a lower radiation effect. Thus, lower temperatures also boosted the convection heat transfer between the black ice surface and the surrounding environment.

The finite element analysis and experiment results are displayed in Figure 20. The temperature in the middle of the surface was higher than 0°C is considered the time to melt black ice. In general, the lower environmental temperature could prolong the melting time of black ice. These outcomes were consistent with the melting area results. The energy from the infrared bulb was absorbed by the environment through convection heat transfer.

## Conclusions

The current study aims to detect black ice formation using a rain sensor and deep learning method. In addition, several conditions that influence the formation process of black ice were considered, including humidity, temperature, water retained on the surface as well as air voids of asphalt concrete. Some key findings are drawn below.

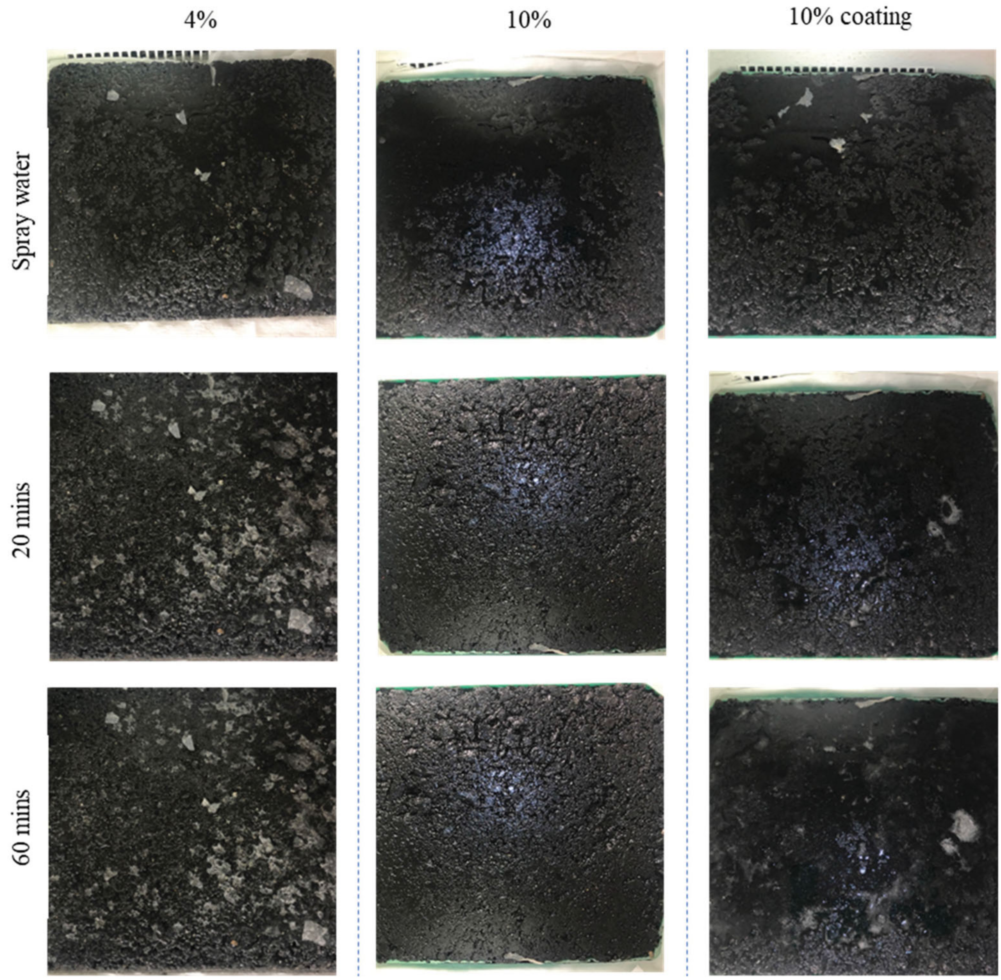


**Figure 18.** Effect of air voids on black ice formation.

- Using a rain sensor to measure black ice formation is very promising, due to the different electrical conductivity between ice and water. The resistance value of the rain sensor increased with cooling time.
- VGG-16 was successfully developed to predict black ice based on image analysis with an accuracy of 90%. In addition, a mobile application was developed using a trained model.
- The humidity lightly affects the formation process of black ice. The higher humidity contributed to a slightly faster formation of black ice. However, the effect of humidity can be negligible.
- It was obvious that the lower temperature leads to a faster black ice formation process. The decrease from −5°C to −15°C could increase 1.5 times the black ice formation process.
- The air voids of asphalt pavement as well as the water content on the surface of pavement act an important role in the formation process of black ice. The higher air void content could reduce the formation of black ice. Environmental also contributed to the melting of black ice, the higher temperature leads to a faster melting time as well as a larger melting area.
- The weather conditions and the pavement types impose a strong impact on the training accuracy. Among them, a foggy environment leads to a noticeable drop in black ice detection effectiveness.

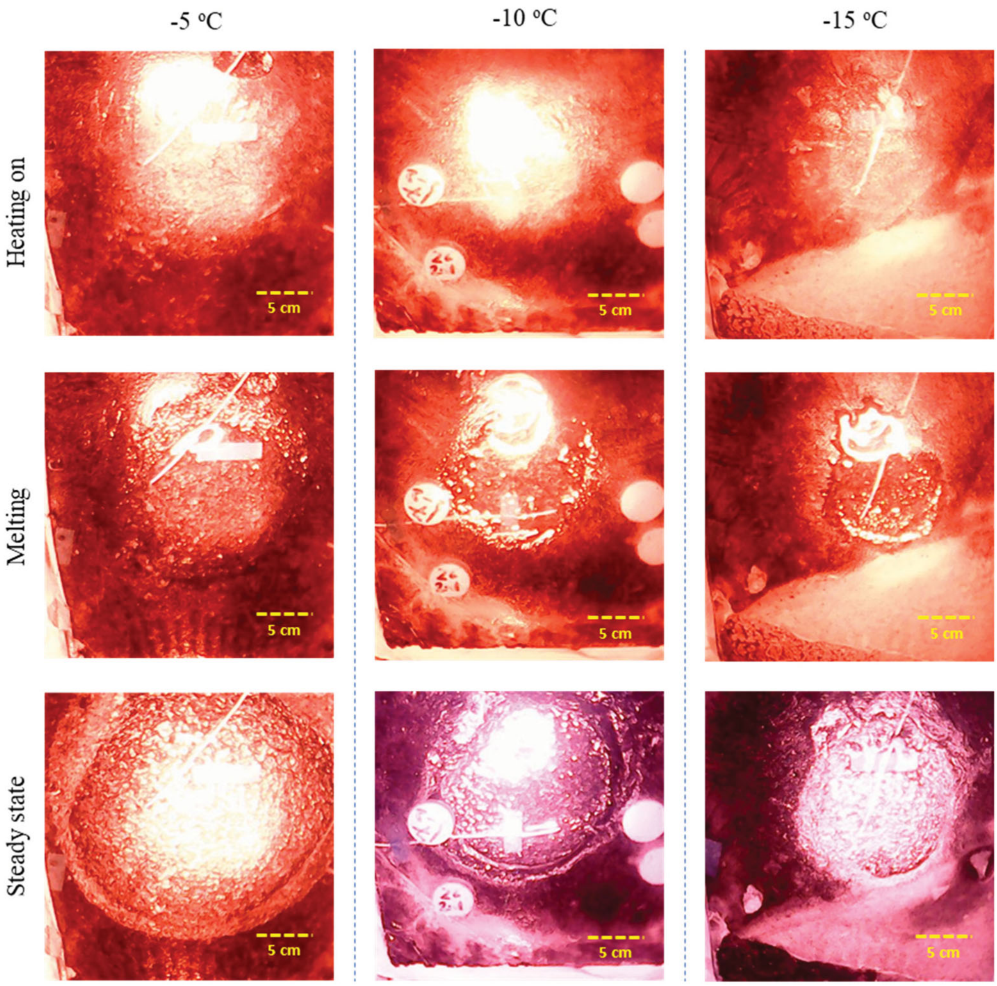


**Figure 19.** Melting by infrared heating.

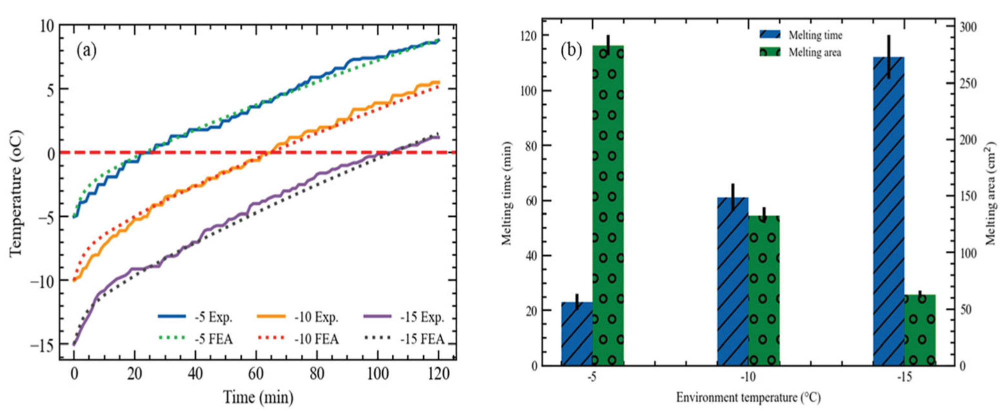


**Figure 20.** Infrared melting experiment and finite element analysis.

- The accuracy results indicated that the performance of different image segmentation models is neglectable. The results showed that the R101-FPN model achieves a better result in the train speed compared to the remained image segmentation models.

In general, the outcomes from this study may be beneficial in developing prediction as well as a melting system using a rain sensor, image analysis and infrared heating. Due to the limited scope of the current study, it is recommended that deep research on environmental conditions such as wind speed should be considered in a further study.

## Disclosure statement

No potential conflict of interest was reported by the author(s).

## Funding

This work was supported by Korea Agency for Infrastructure Technology Advancement (KAIA) grant funded by the Ministry of Land, Infrastructure and Transport [grant number RS-2021-KA161698].

## ORCID

*Tam Minh Phan* http://orcid.org/0000-0001-8696-9207

## References

Arduino. (2019). *How to Use a Rain Sensor*. Arduino. https://create.arduino.cc/projecthub/MisterBotBreak/how-to-use-a-rain-sensor-bcecd9

Bradley, R. S. (1957). The electrical conductivity of ice. *Transactions of the Faraday Society*, *53*(0), 687–691. https://doi.org/10.1039/tf9575300687

Casselgren, J., Sjödahl, M., & LeBlanc, J. P. (2012). Model-based winter road classification. *International Journal of Vehicle Systems Modelling and Testing*, *7*(3), 268–284. https://doi.org/10.1504/IJVSMT.2012.048941

Han, S., Wei, H., Jiang, B., Wang, H., & Chen, J. (2022). Numerical and outdoor experimental study on active snow melting of conductive rubber composites in roads. *Road Materials and Pavement Design*, 1–17. https://doi.org/10.1080/14680629.2022.2103020

Hyun-bin, K. (2019). Fears of black ice spreads nationwide. *The Korea Times*.

Lee, H., Hwang, K., Kang, M., & Song, J. (2020). Black ice detection using CNN for the prevention of accidents in automated vehicle. *2020 International conferenceon computational science and computational intelligence* (*CSCI*), Las Vegas, NV, USA (pp. 1189–1192). https://doi.org/10.1109/CSCI51800.2020.00222

Lee, H., Kang, M., Song, J., & Hwang, K. (2020). The detection of black ice accidents for preventative automated vehicles using convolutional neural networks. *Electronics*, *9*(12), 2178. https://doi.org/10.3390/electronics9122178

Ma, X., & Ruan, C. (2020). Method for black ice detection on roads using tri-wavelength backscattering measurements. *Applied Optics*, *59*(24), 7242–7246. https://doi.org/10.1364/AO.398772

Majidifard, H., Jahangiri, B., Rath, P., Alavi, A. H., & Buttlar, W. G. (2021). A deep learning approach to predict Hamburg rutting curve. *Road Materials and Pavement Design*, *22*(9), 2159–2180. https://doi.org/10.1080/14680629.2021.1886160

Minh Phan, T., Park, D.-W., & Ho Minh Le, T. (2021). Improvement on rheological property of asphalt binder using synthesized micro-encapsulation phase change material. *Construction and Building Materials*, *287*, 123021. https://doi.org/10.1016/j.conbuildmat.2021.123021

Okada, T., Iitaka, T., Yagi, T., & Aoki, K. (2014). Electrical conductivity of ice VII. *Scientific Reports*, *4*(1), 5778. https://doi.org/10.1038/srep05778

Pham, V., Pham, C., & Dang, T. (2020). Road damage detection and classification with Detectron2 and faster R-CNN. *2020 IEEE International conference on big data (big data)*, Atlanta, GA, USA (pp. 5592–5601). https://doi.org/10.1109/BigData50022.2020.9378027

Phan, T. M., Park, D.-W., & Kim, H.-S. (2022). Utilization of micro encapsulated phase change material in asphalt concrete for improving low-temperature properties and delaying black ice. *Construction and Building Materials*, *330*, 127262. https://doi.org/10.1016/j.conbuildmat.2022.127262

Simonyan, K.Z.A. (2015). *Very deep convolutional networks for large-scale image recognition*. Computer Vision and Pattern Recognition.

Singh, J,S,S. (2018). *Road damage detection And classification In smartphone captured images using mask R-CNN*. Computer Vision and Pattern Recognition.

Szklarek, S., Górecka, A., & Wojtal-Frankiewicz, A. (2022). The effects of road salt on freshwater ecosystems and solutions for mitigating chloride pollution – a review. *Science of The Total Environment*, *805*, 150289. https://doi.org/10.1016/j.scitotenv.2021.150289

Tong, Z., Gao, J., Han, Z., & Wang, Z. (2018). Recognition of asphalt pavement crack length using deep convolutional neural networks. *Road Materials and Pavement Design*, *19*(6), 1334–1349. https://doi.org/10.1080/14680629.2017.1308265

Valldorf, J., & Gessner, W. (Eds.). (2007). *Networking sensors and actuators for a New active headrest BT – advanced microsystems for automotive applications* 2007 (pp. 37–46). Springer. https://doi.org/10.1007/978-3-540-71325-8_4

Vo, H. V., Park, D.-W., & Dessouky, S. (2015). Simulation of snow melting pavement performance using measured thermal properties of graphite-modified asphalt mixture. *Road Materials and Pavement Design*, *16*(3), 696–706. https://doi.org/10.1080/14680629.2015.1020847

Zhang, H., Azouigui, S., Sehab, R., & Boukhnifer, M. (2022). Near-infrared LED system to recognize road surface conditions for autonomous vehicles. *Journal of Sensors and Sensor Systems*, *11*(1), 187–199. https://doi.org/10.5194/jsss-11-187-2022

Zhao, W., Wang, L., Zhang, Y., Cao, X., Wang, W., Liu, Y., & Li, B. (2021). Snow melting on a road unit as affected by thermal fluids in different embedded pipes. *Sustainable Energy Technologies and Assessments*, *46*, 101221. https://doi.org/10.1016/j.seta.2021.101221